

Sulphur and biothiol metabolism determines toxicity responses and fate of mercury in *Arabidopsis*

Juan Sobrino-Plata¹, Angel Baron¹, Cristina Ortega-Villasante¹, Victor Ortega-Campayo², Cesar González-Berrocal¹, Carlos Conesa¹, Sandra Carrasco-Gil³, María Muñoz-Pinilla³, Javier Abadia³, Ana Alvarez-Fernandez³, and Luis E. Hernandez¹

¹Universidad Autonoma de Madrid

²Universidad Autonoma de Madrid-Cantoblanco Campus

³Aula Dei Research Experimental Station-CSIC

June 2, 2020

Abstract

Mercury (Hg) is one of the most hazardous pollutants released by humans and is of global environmental concern. Mercury causes oxidative stress and strong cellular damages in plants, which can be attenuated by the biosynthesis of thiol-rich peptides (biothiols), which include glutathione (GSH) and phytochelatins (PCs). We analysed Hg tolerance and speciation in five *Arabidopsis thaliana* genotypes, the wild-type Col-0, three knockdown γ -glutamylcysteine synthetase (γ ECS) mutants and a knockout PC synthase (PCS) mutant. Mercury-PC complexes were detected in roots by HPLC-ESI-TOFMS, with its abundance being limited in γ ECS mutants. Analysis of Hg-biothiol complexes in the xylem sap revealed that HgPC₂ occurs in wild-type Col-0 *Arabidopsis*, suggesting that Hg could be translocated associated with thiol-rich metabolites. Twenty genes involved in sulphur assimilation, GSH and PCs synthesis were differentially expressed in roots and shoots, implying a complex regulation, possibly involving post-translational mechanisms independent of GSH cellular levels. In summary, the present study describes the importance of biothiol metabolism and adequate GSH levels in Hg tolerance, and identifies for the first time Hg-PC complexes in the xylem sap. This finding supports that Hg-biothiol complexes could contribute to Hg mobilisation within plants.

Introduction

The often indiscriminate use of mercury (Hg) in several human activities, mostly related with chemical industries and gold-mining, and the use of ineffective waste removal practices has caused a progressive contamination of soils and groundwater worldwide (Selin, 2010). Contamination by this hazardous metal needs to be tackled by using costly cleaning approaches that result in numerous environmental side effects (Chaney et al., 1997), whereas plant innate ability to take up metals can be exploited for soil phytoremediation (Krämer, 2005), in a sustainable low cost manner particularly appealing in Hg polluted areas (He et al., 2015). However, this requires tolerant plants able to withstand cellular damages caused by toxic metal(loid)s (Rascio & Navari-Izzo, 2011). Among other mechanisms, Hg and other toxic metal(loid)s activate the rapid synthesis of thiol-rich peptides (biothiols) such as glutathione (GSH; γ Glu-Cys-Gly) and phytochelatins (PC; (γ Glu-Cys)_n-Gly, n ranging from 2 to 11) (Cobbett, 2000). Biothiols play a critical role in toxic metal tolerance by maintaining the intracellular redox balance and binding toxic metals to form less harmful chemical species (Hernández et al., 2015), which are translocated to vacuoles limiting the cytosolic concentration of free metal (Sharma, Dietz, & Mimura, 2016). Sulphur assimilation and biothiol metabolism are thought to contribute to Hg tolerance and homeostasis (Carrasco-Gil et al., 2011), but there is still limited knowledge on regulatory mechanisms and how those metabolites mitigate Hg-induced stress.

The overall sulphur acquisition and assimilation pathway is highly conserved in the course of evolution,

determined by ICP-MS NexION 300 Perkin-Elmer Sciex (San Jose, CA, USA).

Σεχυσενσινγ ανδ αλιγνμεντ οφ γE^α μυταντς

Genomic DNA was isolated from the shoots of Col-0, *cad2-1*, *pad2-1* and *rax1-1* plants using the illustra DNA Extraction Kit PHYTOPURE (GE Healthcare Life Sciences), and DNA concentration was measured in a NanoDrop[®] ND-1000 spectrophotometer (Technologies Inc., Wilmington, DE, USA). A 637 bp fragment of gene GSH1 (γ -glutamylcysteine synthetase, γ -ECS) was amplified by PCR using primers γ ECS01F (CGTTTCGGATTATTTCTTGGTGT) and γ ECS02R (GCGGTCCTTGTCAGTGTCTGT), and sequenced in an ABI Prism[®] 3730/3730xl DNA Sequencer (Certified Scientific Instruments, Inc., USA). Sequences were revised and aligned using the Geneious Pro 5.5.3 software in comparison with GSH1 gene sequence (AT4G23100), and the identity of each mutant was verified as described in literature (Supplementary Fig. 1).

RNA extraction and quantification

Total RNA from shoots and roots of *Arabidopsis* was isolated with TRI Reagent (Ambion), cleaned using in-column DNase treatment with the RNeasy Mini Kit (Qiagen) (Montero-Palmero, Martín-Barranco, Escobar, & Hernández, 2013), and quantified in a NanoDrop[®] ND-1000 spectrophotometer (Technologies Inc.). RNA integrity was determined with an Agilent 2100 Bioanalyzer equipped with an RNA 6000 Nano LabChip Kit (Agilent Technologies, Santa Clara, CA, USA) using the RNA integrity number (RIN) algorithm of three independent biological replicates (Schroeder et al., 2006), which showed satisfactory RNA quality in all samples, particularly in those prepared from Hg-treated plants (Supplementary Fig. 2).

Quantitative reverse transcription polymerase chain reaction (qRT-PCR)

Quantitative reverse transcription (RT)-PCR was performed with RNA from *Arabidopsis* shoots and roots in two completely independent biological experiments (three RNA biological replicates each) to synthesize the complementary DNA strand. The RT reaction was performed with random hexamers, using the RETROscript(r) First Strand Synthesis Kit (Applied Biosystems-Life technologies, Carlsbad, CA, USA). Quantitative PCR was carried out with 50 ng single-stranded cDNA in a final volume of 20 μ L, containing 10 μ L of SYBR-Green Master Mix (Applied Biosystems-Life Technologies) and 250 nM forward and reverse specific primers (Life Technologies, Supplementary Table 1), using a Real-Time 7000SDS Thermocycler (Applied Biosystems-Life Technologies), with denaturation at 95 °C for 10 min, 40 cycles of 15 seconds at 95 °C and 1 min annealing and extension at 60 °C. Gene expression was quantified by using the relative 2- $\Delta\Delta$ Ct method (Livak & Schmittgen, 2001), and the glyceraldehyde 3-phosphate dehydrogenase gene (*GAPDH*) as reference (Montero-Palmero et al., 2013).

Glutathione reductase *in gel* activity

GR enzymatic activities were determined *in gel* after separation of protein extracts using non-denaturing polyacrylamide electrophoresis (Sobrino-Plata et al., 2009). Protein loading was 20 and 10 μ g for shoot and root samples, respectively. The staining solution was 250 mM Tris-HCl buffer, pH 7.5, supplemented with 0.2 mg mL⁻¹ thiazolyl blue tetrazolium bromide, 0.2 mg mL⁻¹ 2,6-dichlorophenol indophenol, 0.5 mM NADPH and 3.5 mM GSSG.

Western-blot immunodetection

Immunodetection was performed by Western-blot after denaturing gel electrophoresis (Laemmli, 1970) and blotting onto a nitrocellulose membrane (BioTrace[®]NT Pall Corporation, East Hills, NY, USA), using a semi-dry procedure (Trans Blot[®] SD Semi-Dry Electrophoretic Transfer Cell; BioRad, Hercules, CA, USA). Membranes were incubated overnight at 4°C with the primary antibodies (α -GR (AS06 181), dil. 1/5000; α -gECS (AS06 186), dil. 1/2500 (Agrisera, Vännäs, Sweden). After incubation with the anti-rabbit secondary antibody linked to horse radish peroxidase (HRP), proteins were detected using the LumiSensor Chemiluminescent HRP Substrate Kit (GenScript, Piscataway, NJ, USA), and images were taken with a ChemiDoc XRS+ System (BioRad).

Xylem sap extraction and collection

Plants were collected and roots rinsed with distilled water, then excised at the caulinar (floral) stem above the rosette leaves, and the xylem sap was collected directly from the cut with a micropipette. To improve xylem sap exudation in Hg-stressed plants, roots were subjected to external pressure in a portable SKPM 1400 Scholander pressure chamber (SKYE Instruments Ltd., Powys, UK) by applying a 3 MPa constant pressure with compressed N₂ gas for less than 20 min. The first 10 μ L were discarded to avoid cellular contamination, and the xylem sap collected (45 μ L) was transferred to Eppendorf tubes containing 5 μ L of acid mixture (10% metaphosphoric acid, 1% formic acid and 10 mM EDTA), for preservation of biethiol and biethiol-Hg complexes. Samples were subsequently frozen at -80°C and stored until analysis. Cross-contamination with cellular and phloem exudates was checked routinely by measuring L-malate dehydrogenase (c-MDH) activity (López-Millán, Morales, Abadía, & Abadía, 2000) (see Extended Materials and Methods details in Supplementary online material).

Analysis of biethiols by HPLC-DAD

Biethiols in shoots and roots were analysed by HPLC-UV-diode array detector (DAD) (Sobrinho-Plata et al., 2009). Extracts (100 μ L) were injected in a Mediterranea SEA18 column (5 μ m, 250 x 4.6 mm; Teknokroma, San Cugat del Vallés, Spain), using a 1200 HPLC system (Agilent), and biethiols were detected after post-column derivatization with Ellman reagent. Quantification was carried out adding N-acetyl cysteine (N-AcCys; final concentration 250 μ M) as internal standard prior to sample homogenization.

Analysis of biethiols and ascorbate by HPLC-ESI-MS(TOF)

Ascorbate, biethiols and Hg-biethiol complexes were analysed by HPLC-electro spray ionisation (ESI)-time-of-flight mass spectrometry [MS(TOF)], using an HPLC system (Alliance 2795, Waters, Milford, MA, USA), equipped with a reverse-phase monolithic UPLC column (Mediterranea SEA18 3 μ m 15 x 0.21 cm, Teknokroma), and coupled to a MS-TOF spectrometer (MicroTOF, Bruker Daltonics, Bremen, Germany) equipped with an ESI source (Carrasco-Gil *et al.*, 2011), with a mobile phase made with solvents A (0.1% formic acid in miliQ water), and B (0.1% formic acid in acetonitrile)(see Extended Materials and Methods details in Supplementary online material). After chromatographic separation, sample was directed with a flow rate of 200 μ L min⁻¹ to the ESI interface. The MS(TOF) operated in negative/positive ion mode at -500/4500 V endplate and spray tip voltages, respectively. The orifice voltage was set at 100 V and full scan data acquisition was carried out from m/z 50 to 1000. The mass axis was calibrated externally using Li-formate adducts (10 mM LiOH, 0.2% (v/v) formic acid and 50% (v/v) 2-propanol). The HPLC-ESI-MS(TOF) system was controlled with MicroTOF Control v.2.2 and HyStar v.3.2, and data were managed with Data Analysis v.3.4 (software packages from Bruker Daltonics). Ion chromatograms were extracted with a precision of 0.05 m/z units.

MS/MS for HgPC₂ complex analysis

For LC-MSⁿ measurements the same HPLC system described above is used, including chromatographic column and analysis conditions, but the MSⁿ study was performed using a HCT Ultra high-capacity ion trap (Bruker Daltonics). ESI conditions were as described previously and to establish the optimum MSⁿ conditions, standard solutions of HgPC₂ were tested. A volume of 20 μ L of standard or xylem sap samples was injected into the LC system and MSⁿ analysis were controlled by HyStar v 3.2 software (Bruker Daltonics). MSⁿ experiments were conducted by selecting the high intensity peak mother ion (740.1 m/z for MS, and 536.1 m/z for MS²) at the retention time of the compound chromatographic peak, and data were collected in total ion counting mode, acquiring the spectra in the range 100-1100 m/z .

Statistics

Statistical analysis was performed with SPSS for Windows (v. 19.0), using an ANOVA with Tuckey test. Results shown are means of at least three replicates \pm standard deviation, using $p < 0.05$ to detect statistically significant differences.

RESULTS

Biothiol concentrations in roots and shoots varied greatly depending on *Arabidopsis* genotypes according to the HPLC-DAD analysis (Fig. 1; Supplementary Table 2). Glutathione was present in all genotypes, but it was at remarkably low concentrations in the γ ECS mutants *cad2-1*, *pad2-1* and *rax1-1*, when compared with the levels of the wild type Col-0 (all mutants were unequivocally identified by PCR amplification and sequence alignment; Supplementary Fig. 3). In the phytochelatin-defective mutant *cad1-3*, the GSH concentration in shoots was almost 2-fold compared with the wild-type. In the presence of 3 μ M Hg, PC₂ ((γ Glu-Cys)₂-Gly), PC₃ ((γ Glu-Cys)₃-Gly) and PC₄ ((γ Glu-Cys)₄-Gly) were found in Col-0 roots, whereas only PC₂ and PC₃ appeared in *rax1-1* roots. However, none of those PCs were observed in *cad2-1* and *pad2-1* mutants. As expected, we could not detect PCs in *cad1-3* under Hg stress, in spite of the fact that GSH concentrations were the highest observed both in shoots and roots, doubling the concentration found in *Arabidopsis* Col-0 (Fig. 1; Supplementary Table 2).

The decrease of GSH levels in *pad2-1*, *cad2-1* and *rax1-1* and the inability to synthesize PCs in *cad1-3* were accompanied by significant changes in ascorbic acid (ASA), reduced (GSH) and oxidized glutathione (GSSG) concentrations, as measured by HPLC-ESI-MS(TOF) (Table 1). *Arabidopsis* mutants treated with 3 μ M Hg had ASA concentrations in roots well above of values found in Col-0, which almost doubled in shoots. On the other hand, GSH concentrations followed the same pattern found using HPLC-DAD, with *pad2-1*, *cad2-1* and *rax1-1* having the lowest values both in roots and shoots, whereas the GSH concentration in *cad1-3* was 2-fold higher than Col-0. Exposure to 3 μ M Hg led to general increases in GSH concentrations in shoots and roots of all mutant genotypes, effect particularly intense in *cad1-3*. With respect to GSSG, concentrations were one order of magnitude lower than those of GSH, but they changed with a similar pattern. As a result, there were minimal changes in the relative content of GSSG irrespective of genotype and occurrence of Hg stress.

The marked changes in ASA and GSH/GSSG contents observed in response to Hg suggested possible alterations in the redox balance of mutant shoots and roots. We firstly analysed the concentrations of Hg in shoots and roots of *Arabidopsis*, which accumulated largely in roots (shoots Hg concentrations was less than 1% of that found in roots; Fig. 2a). All γ ECS mutants had similar Hg levels in roots, which were approximately 50% of the concentration found in Col-0 and *cad1-3* plants (Fig. 2a). However, Hg concentrations in shoots were not statistically different between genotypes. In parallel, we determined chlorophyll fluorescence parameters, and observed that non-photochemical quenching was severely impaired in γ ECS and PCS mutant genotypes both in control and 3 μ M Hg-treated plants (Fig. 2b), confirming that limiting biothiols metabolism led to stress in leaves. GR activity, an enzyme specifically sensitive to this Hg (Sobrino-Plata et al. 2009), was not affected in roots (Fig. 3a), but was impaired by Hg in Col-0 and *cad1-3* roots with an almost complete inhibition in *cad2-1*, *pad2-1*, and *rax1-1* mutants (Fig. 3a). Despite such inhibition, the amount of GR protein did not change appreciably in shoots and roots even under Hg-stress independently of the genotype (Fig. 3b). With regard to γ ECS in shoots, protein accumulation under control conditions was remarkably lower (40-50%) in γ ECS and *cad1-3* mutants than in Col-0. Mercury stress also led to a marked decrease in Col-0 leaves, reaching similar values in all genotypes (Fig. 3b). However, there were no differences among genotypes and Hg stress levels in root γ ECS, probably due to the low signal obtained by α - γ ECS immunodetection (high background; Fig. 3b).

Our previous study established that part of the ability of plants to withstand Hg toxicity depends on the formation of Hg-PCs complexes, such as HgPC₂ (Hg(γ GluCys)₂Gly) and HgPC₃ (Hg(γ GluCys)₃Gly) (Carrasco-Gil et al., 2011). Full HPLC-ESI-MS(TOF) analysis of biothiol ligands and Hg-biothiol complexes (Hg-PCs) in shoots and roots of showed clear differences between all studied *Arabidopsis* genotypes (Fig. 4). In shoots, we could only detect free PC₂ ([PC₂-H]⁻; *m/z* 538.1) and PC₃ ([PC₃-H]⁻; *m/z* 770.2) ligands, whereas in roots there were oxidized variants of free PCs, such as ([PC₃oxd-H]⁻; *m/z* 768.2), Hg-PC complexes like HgPC₂ ([HgPC₂-H]⁻; *m/z* 738.1) and HgPC₃ ([HgPC₃-H]⁻; *m/z* 970.1). The graphical table included in Fig. 4b shows the groups of free ligands, oxidised PCs and Hg-biothiol complexes, found in shoots and roots of all *Arabidopsis* genotypes. The results in *rax1-1* and *cad2-1* roots closely resembled those found for Col-0,

where we detected $[\text{HgPC}_2\text{-H}]^-$ and $[\text{HgPC}_3\text{-H}]^-$, albeit with a rather weak signal (data not shown). On the other hand, in *pad2-1* we only found GSH ($[\text{GSH}+\text{H}]^+$; m/z 308.1) and GSSG ($[\text{GSSG}+\text{H}]^+$; m/z 613.3) in roots and shoots, which were better detected in positive mode, in addition to PC_2 , that was just over the background signal. As expected, *cad1-3* did not accumulate free PCs or Hg-PCs complexes.

Recent studies indicated that toxic elements (Cd and As) are chelated with PCs in roots impeding translocation to shoots and potentially helping plants to attenuate stress, in a manner that metal(loid)-PCs complexes would mass in root vacuoles (Liu et al., 2010; Mendoza-Cózatl et al., 2008) However, to some extent metal(loid)s may travel to shoots bound to organic ligands such as PCs (Shi et al., 2019). To determine whether Hg had a similar behaviour, we studied the possible occurrence of biothiols and Hg-PCs complexes in xylem sap by HPLC-ESI-MS(TOF) using both positive and negative modes. Since Hg blocks water movement through plant vascular tissues, we used a Schölander pressure chamber to generate sufficient root pressure to impulse xylem water movement. All xylem sap samples were checked for phloem or broken cells fluids contamination by measuring MDH activity, which indicated that cross-contamination was negligible in all *Arabidopsis* genotypes under Hg stress (Supplementary Fig.3). The compounds GSH ($[\text{GSH}+\text{H}]^+$; m/z 308.1) and GSSG ($[\text{GSSG}+\text{H}]^+$; m/z 613.3) appeared in the xylem sap of all genotypes, albeit signals were lower in γECS mutants (data not shown). The characteristic PC_2 peak ($[\text{PC}_2+\text{H}]^+$; m/z 540.1) appeared in xylem sap of Col-0 and, at very low intensity, also in *rax1-1* (Fig. 5). This compound coeluted with another of m/z 538.1, which was tentatively identified as oxidized PC_2 (PC_2oxd). However, PC_2 or PC_2oxd were not detected in *cad2-1*, *pad2-1* and, as expected, PCS mutant *cad1-3*.

To confirm the nature of PC_2oxd we run in parallel a hydroponic experiment with Col-0 *Arabidopsis* treated with 10 μM Cd for 72 h. In this case, we got a better signal in MS(TOF) in negative mode with a m/z 536.1 ($[\text{PC}_2\text{oxd-H}]^-$) (Supplementary Fig. 4a); molecular ion that was subjected to tandem MS (- MS^2), and was compared with those obtained using PC_2 (m/z 538.13) and PC_2oxd (m/z 536.1) standards, which had characteristic daughter ions at m/z 254.1 and 128.0 (Supplementary Fig. 4c). Incidentally, we were unable to observe any Cd-PC complex, in spite of using ESI-MS(TOF) settings appropriate for detection of CdPC_2 , as we obtained the characteristic peaks associated with the natural Cd isotopic distribution (major $[\text{CdPC}_2\text{-H}]^-$ peak at m/z 650.0) by direct injection of a Cd: PC_2 standard (Supplementary Fig. 4b).

In Col-0 xylem sap, along with to PC_2 and PC_2oxd we found only a compound with the characteristic Hg-isotopic fingerprint that could correspond to Hg-PCs complexes, which was tentatively assigned to HgPC_2 , eluting separately from free bi thiol ligands (Fig. 5a). The MS(TOF) spectrum (in positive mode) of the detected compound ($[\text{HgPC}_2+\text{H}]^+$; m/z 740.1) fitted well with theoretical data and also with a Hg: PC_2 standard mixture (1:1) (Fig. 5b). The identity of the m/z 740.1 ion peak of Col-0 xylem samples was confirmed using tandem MS/MS analysis. The same Hg: PC_2 standard mixture was used to set up analytical conditions, and the m/z 740.1 mother ion was selected and sent to the collision cell for fragmentation (MS^2). Several major daughter ions appeared with m/z 609.1, 536.1 and 508.1 both in the HgPC_2 standard and the Col-0 xylem sap (Fig. 5c). Some of these ions were tentatively identified by comparing with those detected in Hg-bi thiol complexes analysis as follows: m/z 609.1 was assigned to $[\text{HgPC}_2\text{-Glu}]^+$; m/z 536.1 matched $[\text{PC}_2\text{oxd-2H}]^+$, and m/z 508.1 was assigned to $[\text{HgGSH}+\text{H}]^+$. Further identification of the m/z 536.1 ion, with the highest intensity peak, was obtained after a second fragmentation (MS^3) resulting in various ions. The MS^3 spectra of both the xylem sap and the standard mixture were also very similar, with a major m/z 507.1 daughter ion (possibly $[\text{GSH-H}]^+$), with a second m/z 489.1 ion also present in both samples (Fig. 5d). Therefore, we can assert that HgPC_2 complexes could be transferred from roots to shoots *via* xylem flux, process that did not occur in *rax1-1*, *cad2-1* and *cad1-3* mutants. Nevertheless, we could not determine to what extent Hg flows to shoots via xylem, since our ICP-MS analysis failed to detect Hg above background levels, probably due to the small volume of sample collected (10-50 μL).

In view of the relevant role that bi thiol metabolism has in tolerance to Hg and Hg speciation in plants, we analysed the expression pattern of 20 genes involved in sulphur uptake, assimilation and incorporation to biothiols under Hg-stress (Gigolashvili & Kopriva, 2014). The expression pattern was organ-dependent, with some genes being over-expressed in the shoots of certain mutants treated with Hg (Fig. 6), whereas in

the roots we only detected gene down-regulation under Hg stress (Fig. 7). Regarding transcription factors in shoots, *MYB28* was induced only in the γ ECS-mutants *cad2-1* and *pad2-1* under Hg exposure, whereas *MYB51* was suppressed in *rax1-1*. On the other hand, both *MYB28* and *MYB51* were down-regulated in roots under Hg-stress, especially in *rax1-1* and *cad1-3* mutants (Fig. 7). We also found significant down-regulation of *SLIM1* in roots of all mutant *Arabidopsis* genotypes (Fig. 7; Suppl. Tables 3 and 4).

Among the genes involved in sulphur incorporation and assimilation in shoots, the sulphur transporter *SULTR1;2* had the highest over-expression in Hg-treated *cad2-1*, *rax1-1* and *cad1-3* plants, whereas a strong repression was observed in Col-0 (Fig. 6; Suppl. Table 3). A similar repression appeared in Col-0 for ATP sulphurylase (*ATPS3*) and APS reductase (*APR1* and *APR3*) (Fig. 6). On the other hand, *ATPS4* (only in *pad2-1*), *APR1*, *APR2* and *APR3* (only in *rax1-1*), were over-expressed in *pad2-1*, *rax1-1* and *cad1-3* plants treated with 3 μ M Hg. With regard to GSH and PCs metabolism, we only observed a minor down-regulation under Hg stress, particularly significant for *cad2-1* and *pad2-1* O-acetylserine (thiol) lyase (*OASTLA* and *OASTLB*) genes. Interestingly, expression of the phytochelatin synthase genes *PCS1* and *PCS2* decreased in leaves in Hg-treated plants, being particularly significant in *pad2-1*, *rax1-1* and *cad1-3* (Fig. 6, Supplementary Table 3). Finally, in roots under Hg stress we only observed significant gene down-regulation, mostly in the mutant genotypes. Especially relevant was the down-regulation of sulphate transporters, including a remarkable decrease for *SULTR1;2* in *cad2-1*, *rax1-1* and *cad1-3* (Fig. 7). The expression of other sulphur transporters decreased, including that of *SULTR2;1* in *rax1-1* and *cad1-3*, and *SULTR3;5*, which was very intense in all Hg-exposed *Arabidopsis* genotypes. With regard to sulphur assimilation genes, the most consistent changes occurred in *cad1-3*, where *ATPS1*, *ATPS3*, *SiR*, *OASTLB*, *OASTLC*, γ E Σ , *GSH-S*, *PCS1* and *PCS2* expression decreased in plants treated with 3 μ M Hg (Fig. 7, Supplementary Table 4).

DISCUSSION

Knock-down of γ ECS resulted in a drastic limitation of biothiol concentrations under control and Hg-stress conditions, particularly in the *cad2-1* and *pad2-1* mutants (Fig. 1), confirming previous results in these GSH-depleted genotypes (Parisy et al., 2007; Ball et al., 2004; Cobbett, 2000) and in *Arabidopsis* leaf discs and plants treated with similar doses of Hg and Cd (Sobrinho-Plata et al., 2014a; 2014b). Interestingly, the mildly-affected knock-down *rax1-1* γ ECS mutant treated with 3 μ M Hg also accumulated PC₂ and PC₃ (but not PC₄) in roots, but to a lower extent than did wild-type plants as observed in Cd-treated plants (Sobrinho-Plata et al., 2014b). We were unable to detect PCs in shoots, organs that accumulated much less Hg than roots (by two orders of magnitude), since a certain Hg concentration threshold may be required to trigger synthesis of PCs. In fact, numerous PCs appeared in Col-0 and *rax1-1* leaf discs subjected to direct infiltration with 3 and 30 μ M Hg; behaviour that was accentuated at longer exposure times (48 h) when PC₂ and PC₃ also appeared in *cad2-1* (Sobrinho-Plata et al., 2014a). On the other hand, the inability to synthesize PCs in *cad1-3* led to a significantly higher GSH accumulation in when compared to Col-0 (Fig. 1, Table 1). Interestingly, this increase became larger under Hg stress, in agreement with our previous observations in *cad1-3* leaf discs infiltrated with 3 μ M Hg for 24 h (Sobrinho-Plata et al., 2014a). It has been proposed recently that PCS functions as a transpeptidase important for GSH and conjugated GSH turnover, which may explain the high GSH levels found in *cad1-3* plants (Kühnlenz, Westphal, Schmidt, Scheel, & Clemens, 2015).

Depletion of GSH resulted in the elicitation of a severe oxidative stress with 3 μ M Hg, with a marked inhibition of GR activity in the roots of γ ECS mutants in comparison with Col-0 and *cad1-3*, without any changes in enzyme amount (Fig. 3). The mutant *cad1-3* lacked the ability to form Hg-PC complexes, but the Hg-induced damage was similar to that found in Col-0, possibly due to enhanced GSH levels in this mutant. Strong GR inhibition occurred in roots of *cad2-1*, *pad2-1* and *rax1-1* treated with 10 μ M Hg for 72 h, which also suffered extensive alterations in membrane proteins (i.e., degradation of H⁺-ATPase and strong inhibition of NADPH-oxidase; Sobrinho-Plata et al., 2014b). The GR inhibition appears to be triggered specifically by Hg over certain concentrations in *Medicago sativa* or *Silene vulgaris*, whereas other toxic elements usually lead to an enhanced activity (Sobrinho-Plata et al., 2013; 2009), as can be used as a marker of

Hg-stress. Besides the strong GR inhibition, there were minor and non-consistent changes in the proportion of GSSG in the analysed *Arabidopsis* genotypes (Table 1). This concurs with the minimal oxidation of homogluthathione (hGSH) (less than 15%) found in 30 μ M Hg-treated alfalfa seedlings (Ortega-Villasante et al., 2007). Therefore, even though GSH synthesis was compromised in γ ECS mutants, much severe and chronic cellular damage would be required to observe relevant GSH oxidation. On the other hand, the poorer tolerance to Hg caused by limited GSH also led to alterations of chlorophyll fluorescence parameters, with a remarkable NPQ decrease (Fig. 2), in accordance with results obtained in *Arabidopsis* treated with Hg, Cd and Cu over 72 h (Maksymiec, Wójcik, & Krupa, 2007; Sobrino-Plata et al., 2014a). GSH plays a central role in chloroplast redox balance, keeping ASA and xanthophyll pools reduced at optimal levels to sustain NPQ under stress (Yin et al., 2010), which may be hampered in γ ECS mutants. Interestingly, the increase in ASA shoot concentrations under Hg stress was particularly intense in γ ECS mutant genotypes. Similar response was found in Cd-treated *cad2-1* mutants, where ASA concentration was higher than in wild-type plants, particularly in roots (Jozefczak et al., 2015). In this respect, recent experiments showed that increases in ASA concentrations are a common response of plants to metal stress, especially in shoots where this antioxidant metabolite helps protecting the photosynthetic apparatus, which may be hampered by both the lack of GSH and the oxidative stress induced by Hg (Bielen, Remans, Vangronsveld, & Cuypers, 2013).

Mercury is thought to bind strongly to cell walls of epidermal and xylem root cells, possibly bound to the Cys thiol residues of proteins, thus preventing translocation to shoots (Carrasco-Gil et al., 2011; 2013), as found in roots of different plant species (Carrasco-Gil et al., 2011; Sobrino-Plata et al., 2009; 2013; 2014b). Interestingly, γ ECS mutants roots had significant lower Hg concentration than Col-0, with no effects in shoots, whereas stronger Hg-induced damages appeared in the mutants. Similarly, metal accumulation in shoots did not change in Cd- and Hg-treated *cad2-1* plants (Li, Dankher, Carreira, Smith, & Meagher, 2006), in line with the view that cellular biothiol levels have little impact on overall plant metal distribution (Lee et al., 2003). On the other hand, it is known that transpiration is strongly impaired by Hg (Moreno, Anderson, Stewart, & Robinson, 2008), a toxic metal that drastically reduces metabolic-driven water conductance in roots (Lovisolo, Tramontini, Flexas, & Schubert, 2008). Toxic effect that impelled us to use the Schölander pressure chamber to collect enough xylem sap under Hg stress, particularly in γ ECS mutant plants. Therefore, it is feasible that the strong Hg-stress in γ ECS mutants caused poorer water flow to shoots, limiting Hg uptake and translocation to the aerial part of Hg-exposed plants.

Xylem conforms, along with phloem, the major long-distance transport system for movement and distribution of water, ions and metals throughout the plant (Álvarez-Fernández et al., 2014). Cadmium transport by the xylem determines Cd accumulation in shoots, which depends on loading driven by metal transporters (Wu et al., 2015), while biothiols have been suggested as long distance carriers for Cd in the phloem of *Brassica napus* (Mendoza-Cózatl et al., 2008). The high stability of Hg-PC complexes found in plant roots could provide a basis for Hg long-distance transport, as it was suggested by the association of Hg with sulphur in stems and leaf veins of alfalfa plants exposed to Hg (Carrasco-Gil et al., 2013). HPLC-ESI-MS(TOF) analysis revealed for the first time that $[\text{HgPC}_2\text{-H}]^+$ indeed occurs in the xylem sap of Col-0 (Fig. 5), identity that was confirmed by MS^n analysis, with daughter molecular ions in the MS^2 and MS^3 spectra matching those of standards. We also detected free $[\text{PC}_2\text{-H}]^-$ and $[\text{PC}_2\text{oxd-H}]^-$ in xylem sap, confirming our preliminary findings in the xylem sap of Col-0 plants treated with 10 μ M Cd for 72 h (Supplementary Fig. 2). Oxidised PC_2 was also found in the xylem sap of *Brassica napus* plants subjected to Cd (Mendoza-Cózatl et al., 2008) and *Arabidopsis* seedlings treated with As (Liu et al., 2010), but metal(loid)-PC complexes were not found in those cases. Moreover, a very low concentration of As was found in xylem sap of the metallophyte castor bean, which was accompanied again with oxidised GSH and PC_2 (Ye et al., 2010), probably as a result of the oxidative stress and redox imbalance triggered by metal(loid)s. As(III)- and Cd-biothiols complexes may be less stable than those formed with Hg in our conditions, able to withstand even acidic extraction.

Plants treated with metals experience alterations in sulphate uptake and assimilation (Na & Salt, 2011; Nocito et al., 2006), which prompted us to analyse the expression of twenty genes involved in the sulphur assimilatory pathway under Hg-stress. Our results revealed in all *A. thaliana* genotypes tested different responses to Hg in roots and shoots, indicating that both organs had independent stress responses as found with

other metals (Jozefczak et al., 2014). In general, we observed a modest response of genes with fold-changes generally not larger than three (significant at $p < 0.05$), following the same pattern of recent transcriptomic analyses performed after short-term Hg treatments in *Medicago* (Montero-Palmero et al., 2013; Zhou et al., 2013), barley (Lopes et al., 2013), rice (Chen et al., 2014) and tomato (Hou, Liu, Wang, Zhao, & Cui, 2015).

With regard to sulphur metabolism regulation, several transcription factors have been reported to be over-expressed under S-starvation, such as the central hub SLIM1 regulator and several R2R3-MYBs, including MYB28 and MYB51 (Frerigmann & Gigolashvili, 2014). However, we only observed MYB28 upregulation in *cad2-1* and *pad2-1* shoots under Hg stress. Incidentally, a rice R2R3-MYB (OsARM1) has been found to be upregulated in stems and leaves upon As exposure (Wang et al., 2017), and several R2R3-MYBs control response to Cd-stress *via* ABA signalling (Zhang et al., 2019). However, we found marked MYB28, MYB51 and SLIM1 down-regulation in roots of Hg-stressed γ ECS and *cad1-3 Arabidopsis* mutants, which can likely explain the low expression of several sulphur assimilatory pathway genes. Little is known about how SLIM1 may operate under abiotic stress, which may undergo post-transcriptional redox imbalance regulation occurring in Hg-treated γ ECS mutants (Koprivova & Kopriva, 2014).

Sulphate uptake is a bottleneck in plant sulphur incorporation, which were upregulated under metal stress, such as *SULTR1;1* in roots of maize (Nocito et al., 2006) and *Arabidopsis* (Ferri et al., 2017). However, other members of the SULTR transporter gene family in Chinese cabbage plantlets and sorghum responded in different manner in leaves and roots under metal stresses (Shahbaz et al., 2014; Akbudak, Filiz, & Kontbay, 2018). We found that sulphate transporter *SULTR1;2* was up-regulated in shoots in *Arabidopsis* γ ECS and PCS mutants under Hg-stress, response was also found for *SULTR3;5* in roots of *Medicago* just after 6 h exposure to 3 μ M Hg (Montero-Palmero et al., 2013). Conversely, *SULTR1;2* was down-regulated in shoots of Col-0 and roots of all *Arabidopsis* mutants, following the same pattern of *SULTR2;1* and *SULTR3;5* (Figs. 6, 7), in agreement with the short-term down regulation of *SULTR3;3* in rice seedlings treated with 25 μ M Hg for 3 h (Chen et al., 2014). Cadmium exposure and sulphate limitation revealed differences in the transcriptional control of three sulphate transporter (*SULTR1;2*) genes in *Brassica juncea* (Lancilli et al., 2014). Similarly, *SULTR1* and *SULTR2* expression decreased in roots and shoots of Cd-treated *Arabidopsis* at high Cd doses (over 40 μ M) (Yamaguchi et al., 2016). Therefore, *SULTR* expression under metal stress changed depending on the plant organ, supplied metal and doses, implying a complex regulation and specific responses. Time-course experiments to monitor the metal induced expression of *SULTR1;2* showed that in roots it peaked a few hours after metal exposure but subsided subsequently (Jobe et al., 2012). It is feasible that the GSH depletion promoted *SULTR1;2* expression in shoots under Hg stress, where we observed significant redox alterations, whereas under acute cellular damage there might be a general transcriptional down-regulation in roots (Montero-Palmero et al., 2013).

APRs are key enzymes of sulphur assimilatory pathway, that produce sulphite from adenosine 5' phosphosulphate (Kopriva, 2006), genes that were up-regulated in *Arabidopsis* γ ECS and PCS mutants shoots treated with Hg, in agreement with the overexpression found in short-term Hg-treated *Medicago* (Montero-Palmero et al., 2013). However, the rest of S-assimilatory pathway genes in shoots and roots of γ ECS and PCS mutants were modestly affected or down-regulated by Hg (Figs. 6, 7). It must be emphasized that until now none of the transcriptomic analyses carried out in plants treated with Hg showed significant changes in gene expression of enzymes involved in Cys, γ EC, GSH or PCs synthesis (Chen et al., 2014; Hou et al., 2015; Lopes et al., 2013; Montero-Palmero et al., 2013; Zhou et al., 2013). In consequence, despite the several significant changes in S-assimilatory gene expression, occurring mainly in GSH deprived plants, we cannot rule out that the process can be post-transcriptionally controlled. Several stress hormones and the redox cellular balance can contribute to altered enzymatic activities that modify biothiol pools (Kopriva et al., 2019); mechanisms that should be the matter of future research.

In conclusion, depletion of GSH led to stronger Hg toxicity visualised by strong inhibition of GR activity, a poor accumulation of Hg-PC complexes and a limited translocation of HgPC₂ to shoots via xylem transport. Sulphur metabolism and accumulation of biothiols help withstanding Hg-induced oxidative stress, but the mechanisms of regulation remain to be characterised in detail. Although some responses at the transcriptional

level were detected, we cannot rule out post-transcriptional regulation, which probably play a relevant role to procure sufficient biothiols to limit Hg induced damage. In this sense, transcriptional sulphur-assimilation regulation could be independent of GSH cellular levels, in spite of being an essential factor to maintain the cellular redox balance that was compromised by Hg.

REFERENCES

- Akbudak, M. A., Filiz, E., & Kontbay, K. (2018). Genome-wide identification and cadmium induced expression profiling of sulfate transporter (SULTR) genes in sorghum (*Sorghum bicolor* L.). *BioMetals* . <https://doi.org/10.1007/s10534-017-0071-5>
- Álvarez-Fernández, A., Díaz-Benito, P., Abadía, A., López-Millán, A.-F., & Abadía, J. (2014). Metal species involved in long distance metal transport in plants. *Frontiers in Plant Science* . <https://doi.org/10.3389/fpls.2014.00105>
- Ball, L., Accotto, G. P., Bechtold, U., Creissen, G., Funck, D., Jimenez, A., Kular, B., Leyland, N., Mejia-Carranza, J., Reynolds, H., Karpinski, S., & Mullineaux, P. M. (2004). Evidence for a direct link between glutathione biosynthesis and stress defense gene expression in *Arabidopsis* . *Plant Cell* . <https://doi.org/10.1105/tpc.104.022608>
- Bielen, A., Remans, T., Vangronsveld, J., & Cuypers, A. (2013). The influence of metal stress on the availability and redox state of ascorbate, and possible interference with its cellular functions. *International Journal of Molecular Sciences* . <https://doi.org/10.3390/ijms14036382>
- Carrasco-Gil, S., Álvarez-Fernández, A., Sobrino-Plata, J., Millán, R., Carpena-Ruiz, R. O., Leduc, D. L., & Hernández, L. E. (2011). Complexation of Hg with phytochelatin is important for plant Hg tolerance. *Plant, Cell and Environment* . <https://doi.org/10.1111/j.1365-3040.2011.02281.x>
- Carrasco-Gil, S., Siebner, H., Leduc, D. L., Webb, S. M., Millán, R., Andrews, J. C., & Hernández, L. E. (2013). Mercury localization and speciation in plants grown hydroponically or in a natural environment. *Environmental Science and Technology* . <https://doi.org/10.1021/es303310t>
- Chaney, R. L., Malik, M., Li, Y. M., Brown, S. L., Brewer, E. P., Angle, J. S., & Baker, A. J. M. (1997). Phytoremediation of soil metals. *Current Opinion in Biotechnology* . [https://doi.org/10.1016/S0958-1669\(97\)80004-3](https://doi.org/10.1016/S0958-1669(97)80004-3)
- Chen, Y. A., Chi, W. C., Trinh, N. N., Huang, L. Y., Chen, Y. C., Cheng, K. T., Huang, T.L., Lin, C.Y., & Huang, H. J. (2014). Transcriptome profiling and physiological studies reveal a major role for aromatic amino acids in mercury stress tolerance in rice seedlings. *PLoS ONE* . <https://doi.org/10.1371/journal.pone.0095163>
- Cobbett, C. S. (2000). Phytochelatin and their roles in heavy metal detoxification. *Plant Physiology* . <https://doi.org/10.1104/pp.123.3.825>
- Ferri, A., Lancilli, C., Maghrebi, M., Lucchini, G., Sacchi, G. A., & Nocito, F. F. (2017). The sulfate supply maximizing *Arabidopsis* shoot growth is higher under long- than short-term exposure to cadmium. *Frontiers in Plant Science* . <https://doi.org/10.3389/fpls.2017.00854>
- Frigimann, H., & Gigolashvili, T. (2014). Update on the role of R2R3-MYBs in the regulation of glucosinolates upon sulfur deficiency. *Frontiers in Plant Science* . <https://doi.org/10.3389/fpls.2014.00626>
- Gigolashvili, T., & Kopriva, S. (2014). Transporters in plant sulfur metabolism. *Frontiers in Plant Science* . <https://doi.org/10.3389/fpls.2014.00442>
- He, F., Gao, J., Pierce, E., Strong, P. J., Wang, H., & Liang, L. (2015). In situ remediation technologies for mercury-contaminated soil. *Environmental Science and Pollution Research* . <https://doi.org/10.1007/s11356-015-4316-y>
- Hernández, L. E., Sobrino-Plata, J., Montero-Palmero, M. B., Carrasco-Gil, S., Flores-Cáceres, M. L., Ortega-Villasante, C., & Escobar, C. (2015). Contribution of glutathione to the control of cellular redox homeostasis

- under toxic metal and metalloid stress. *Journal of Experimental Botany* . <https://doi.org/10.1093/jxb/erv063>
- Hou, J., Liu, X., Wang, J., Zhao, S., & Cui, B. (2015). Microarray-based analysis of gene expression in lycopersicon esculentum seedling roots in response to cadmium, chromium, mercury, and lead. *Environmental Science and Technology* . <https://doi.org/10.1021/es504154y>
- Jobe, T. O., Sung, D. Y., Akmakjian, G., Pham, A., Komives, E. A., Mendoza-Cózatl, D. G., & Schroeder, J. I. (2012). Feedback inhibition by thiols outranks glutathione depletion: A luciferase-based screen reveals glutathione-deficient γ -ECS and glutathione synthetase mutants impaired in cadmium-induced sulfate assimilation. *Plant Journal* . <https://doi.org/10.1111/j.1365-313X.2012.04924.x>
- Jozefczak, M., Bohler, S., Schat, H., Horemans, N., Guisez, Y., Remans, T., Vangronsveld, J., & Cuypers, A. (2015). Both the concentration and redox state of glutathione and ascorbate influence the sensitivity of *Arabidopsis* to cadmium. *Annals of Botany* . <https://doi.org/10.1093/aob/mcv075>
- Jozefczak, M., Keunen, E., Schat, H., Blik, M., Hernández, L. E., Carleer, R., Remans, T., Bohler, S., Vangronsveld, J., & Cuypers, A. (2014). Differential response of *Arabidopsis* leaves and roots to cadmium: Glutathione-related chelating capacity vs antioxidant capacity. *Plant Physiology and Biochemistry* . <https://doi.org/10.1016/j.plaphy.2014.07.001>
- Khodamoradi, K., Khoshgoftarmansh, A. H., & Maibody, S. A. M. M. (2017). Root uptake and xylem transport of cadmium in wheat and triticale as affected by exogenous amino acids. *Crop and Pasture Science* . <https://doi.org/10.1071/CP17061>
- Kopriva, S., Malagoli, M., & Takahashi, H. (2019). Sulfur nutrition: Impacts on plant development, metabolism, and stress responses. *Journal of Experimental Botany* . <https://doi.org/10.1093/jxb/erz319>
- Kopriva, S. (2006). Regulation of sulfate assimilation in *Arabidopsis* and beyond. *Annals of Botany* . <https://doi.org/10.1093/aob/mcl006>
- Koprivova, A., & Kopriva, S. (2014). Molecular mechanisms of regulation of sulfate assimilation: First steps on a long road. *Frontiers in Plant Science* . <https://doi.org/10.3389/fpls.2014.00589>
- Krämer, U. (2005). Phytoremediation: Novel approaches to cleaning up polluted soils. *Current Opinion in Biotechnology* . <https://doi.org/10.1016/j.copbio.2005.02.006>
- Kühnlenz, T., Westphal, L., Schmidt, H., Scheel, D., & Clemens, S. (2015). Expression of *Caenorhabditis elegans* PCS in the *AtPCS1*-deficient *Arabidopsis thaliana cad1-3* mutant separates the metal tolerance and non-host resistance functions of phytochelatin synthases. *Plant Cell and Environment* . <https://doi.org/10.1111/pce.12534>
- Laemmli, U. K. (1970). Cleavage of structural proteins during the assembly of the head of bacteriophage T4. *Nature* . <https://doi.org/10.1038/227680a0>
- Lancilli, C., Giacomini, B., Lucchini, G., Davidian, J. C., Cocucci, M., Sacchi, G. A., & Nocito, F. F. (2014). Cadmium exposure and sulfate limitation reveal differences in the transcriptional control of three sulfate transporter (*Sultr1;2*) genes in *Brassica juncea*. *BMC Plant Biology* . <https://doi.org/10.1186/1471-2229-14-132>
- Lee, S., Petros, D., Moon, J. S., Ko, T. S., Goldsbrough, P. B., & Korban, S. S. (2003). Higher levels of ectopic expression of *Arabidopsis* phytochelatin synthase do not lead to increased cadmium tolerance and accumulation. *Plant Physiology and Biochemistry* . [https://doi.org/10.1016/S0981-9428\(03\)00140-2](https://doi.org/10.1016/S0981-9428(03)00140-2)
- Li, Y., Dankher, O. P., Carreira, L., Smith, A. P., & Meagher, R. B. (2006). The shoot-specific expression of γ -glutamylcysteine synthetase directs the long-distance transport of thiol-peptides to roots conferring tolerance to mercury and arsenic. *Plant Physiology* . <https://doi.org/10.1104/pp.105.074815>
- Liu, W. J., Wood, B. A., Raab, A., McGrath, S. P., Zhao, F. J., & Feldmann, J. (2010). Complexation of arsenite with phytochelatin reduces arsenite efflux and translocation from roots to shoots in *Arabidopsis* .

Plant Physiology . <https://doi.org/10.1104/pp.109.150862>

Livak, K. J., & Schmittgen, T. D. (2001). Analysis of relative gene expression data using real-time quantitative PCR and the $2^{-\Delta\Delta T}$ method. *Methods* . <https://doi.org/10.1006/meth.2001.1262>

Lopes, M. S., Iglesia-Turiño, S., Cabrera-Bosquet, L., Serret, M. D., Bort, J., Febrero, A., & Araus, J. L. (2013). Molecular and physiological mechanisms associated with root exposure to mercury in barley. *Metallomics* . <https://doi.org/10.1039/c3mt00084b>

López-Millán, A. F., Morales, F., Abadía, A., & Abadía, J. (2000). Effects of Iron Deficiency on the composition of the leaf apoplastic fluid and xylem sap in sugar beet. Implications for iron and carbon transport. *Plant Physiology* . <https://doi.org/10.1104/pp.124.2.873>

Lovisolo, C., Tramontini, S., Flexas, J., & Schubert, A. (2008). Mercurial inhibition of root hydraulic conductance in *Vitis* spp. rootstocks under water stress. *Environmental and Experimental Botany* . <https://doi.org/10.1016/j.envexpbot.2007.11.005>

Maksymiec, W., Wójcik, M., & Krupa, Z. (2007). Variation in oxidative stress and photochemical activity in *Arabidopsis thaliana* leaves subjected to cadmium and excess copper in the presence or absence of jasmonate and ascorbate. *Chemosphere* . <https://doi.org/10.1016/j.chemosphere.2006.06.025>

Maxwell, K., & Johnson, G. N. (2000). Chlorophyll fluorescence - A practical guide. *Journal of Experimental Botany* . <https://doi.org/10.1093/jxb/51.345.659>

Mendoza-Cózatl, D. G., Butko, E., Springer, F., Torpey, J. W., Komives, E. A., Kehr, J., & Schroeder, J. I. (2008). Identification of high levels of phytochelatin, glutathione and cadmium in the phloem sap of *Brassica napus* . A role for thiol-peptides in the long-distance transport of cadmium and the effect of cadmium on iron translocation. *Plant Journal* . <https://doi.org/10.1111/j.1365-313X.2008.03410.x>

Montero-Palmero, M. B., Martín-Barranco, A., Escobar, C., & Hernández, L. E. (2013). Early transcriptional responses to mercury: A role for ethylene in mercury-induced stress. *New Phytologist* . <https://doi.org/10.1111/nph.12486>

Moreno, F. N., Anderson, C. W. N., Stewart, R. B., & Robinson, B. H. (2008). Phytofiltration of mercury-contaminated water: Volatilisation and plant-accumulation aspects. *Environmental and Experimental Botany* . <https://doi.org/10.1016/j.envexpbot.2007.07.007>

Na, G. N., & Salt, D. E. (2011). The role of sulfur assimilation and sulfur-containing compounds in trace element homeostasis in plants. *Environmental and Experimental Botany* . <https://doi.org/10.1016/j.envexpbot.2010.04.004>

Nocito, F. F., Lancilli, C., Crema, B., Fourcroy, P., Davidian, J.-C., & Sacchi, G. A. (2006). Heavy metal stress and sulfate uptake in maize roots. *Plant Physiology* . <https://doi.org/10.1104/pp.105.076240>

Ortega-Villasante, C., Hernández, L. E., Rellán-Alvarez, R., Del Campo, F. F., & Carpena-Ruiz, R. O. (2007). Rapid alteration of cellular redox homeostasis upon exposure to cadmium and mercury in alfalfa seedlings. *New Phytologist* , <https://doi.org/10.1111/j.1469-8137.2007.02162.x>.

Parisy, V., Poinssot, B., Owsianowski, L., Buchala, A., Glazebrook, J., & Mauch, F. (2007). Identification of PAD2 as a γ -glutamylcysteine synthetase highlights the importance of glutathione in disease resistance of *Arabidopsis* . *Plant Journal* . <https://doi.org/10.1111/j.1365-313X.2006.02938.x>

Rascio, N., & Navari-Izzo, F. (2011). Heavy metal hyperaccumulating plants: How and why do they do it? And what makes them so interesting? *Plant Science* . <https://doi.org/10.1016/j.plantsci.2010.08.016>

Schroeder, A., Mueller, O., Stocker, S., Salowsky, R., Leiber, M., Gassmann, M., Lightfoot, S., Menzel, W., Granzow, M. & Ragg, T. (2006). The RIN: An RNA integrity number for assigning integrity values to RNA measurements. *BMC Molecular Biology* . <https://doi.org/10.1186/1471-2199-7-3>

- Selin, N. E. (2010). Global biogeochemical cycling of mercury: A review. *Annual Review of Environment and Resources* . <https://doi.org/10.1146/annurev.environ.051308.084314>
- Shahbaz, M., Stuver, C. E. E., Posthumus, F. S., Parmar, S., Hawkesford, M. J., & De Kok, L. J. (2014). Copper toxicity in Chinese cabbage is not influenced by plant sulphur status, but affects sulphur metabolism-related gene expression and the suggested regulatory metabolites. *Plant Biology* . <https://doi.org/10.1111/plb.12019>
- Sharma, S. S., Dietz, K. J., & Mimura, T. (2016). Vacuolar compartmentalization as indispensable component of heavy metal detoxification in plants. *Plant, Cell and Environment* . <https://doi.org/10.1111/pce.12706>
- Shi, W., Zhang, Y., Chen, S., Polle, A., Rennenberg, H., & Luo, Z. B. (2019). Physiological and molecular mechanisms of heavy metal accumulation in nonmycorrhizal versus mycorrhizal plants. *Plant, Cell and Environment* . <https://doi.org/10.1111/pce.13471>
- Sobrinho-Plata, J., Carrasco-Gil, S., Abadía, J., Escobar, C., Álvarez-Fernández, A., & Hernández, L. E. (2014a). The role of glutathione in mercury tolerance resembles its function under cadmium stress in *Arabidopsis* . *Metallomics* . <https://doi.org/10.1039/c3mt00329a>
- Sobrinho-Plata, J., Meysen, D., Cuypers, A., Escobar, C., & Hernández, L. E. (2014b). Glutathione is a key antioxidant metabolite to cope with mercury and cadmium stress. *Plant and Soil* . <https://doi.org/10.1007/s11104-013-2006-4>
- Sobrinho-Plata, J., Herrero, J., Carrasco-Gil, S., Pérez-Sanz, A., Lobo, C., Escobar, C., Millán, R., & Hernández, L. E. (2013). Specific stress responses to cadmium, arsenic and mercury appear in the metallophyte *Silene vulgaris* when grown hydroponically. *RSC Advances* . <https://doi.org/10.1039/c3ra40357b>
- Sobrinho-Plata, J., Ortega-Villasante, C., Laura Flores-Cáceres, M., Escobar, C., Del Campo, F. F., & Hernández, L. E. (2009). Differential alterations of antioxidant defenses as bioindicators of mercury and cadmium toxicity in alfalfa. *Chemosphere* . <https://doi.org/10.1016/j.chemosphere.2009.08.007>
- Tocquin, P., Corbesier, L., Havelange, A., Pieltain, A., Kurtem, E., Bernier, G., & Perilleux, C. (2003). A novel high efficiency, low maintenance, hydroponic system for synchronous growth and flowering of *Arabidopsis thaliana* . *BMC Plant Biology* . <https://doi.org/10.1186/1471-2229-3-2>
- Wang, F. Z., Chen, M. X., Yu, L. J., Xie, L. J., Yuan, L. B., Qi, H., Xiao, M., Guo, W., Chen, Z., Yi, K., Zhang, J., Qiu, R., Shu, W., Xiao, S., & Chen, Q. F. (2017). OsARM1, an R2R3 MYB Transcription factor, is involved in regulation of the response to arsenic stress in rice. *Frontiers in Plant Science* . <https://doi.org/10.3389/fpls.2017.01868>
- Wu, Z., Zhao, X., Sun, X., Tan, Q., Tang, Y., Nie, Z., & Hu, C. (2015). Xylem transport and gene expression play decisive roles in cadmium accumulation in shoots of two oilseed rape cultivars (*Brassica napus*). *Chemosphere* . <https://doi.org/10.1016/j.chemosphere.2014.09.099>
- Yamaguchi, C., Takimoto, Y., Ohkama-Ohtsu, N., Hokura, A., Shinano, T., Nakamura, T., Suyama, A., & Maruyama-Nakashita, A. (2016). Effects of cadmium treatment on the uptake and translocation of sulfate in *Arabidopsis thaliana* . *Plant and Cell Physiology* . <https://doi.org/10.1093/pcp/pcw156>
- Ye, W. L., Wood, B. A., Stroud, J. L., Andralojc, P. J., Raab, A., McGrath, S. P., Feldmann, J., & Zhao, F. J. (2010). Arsenic speciation in phloem and xylem exudates of castor bean. *Plant Physiology* . <https://doi.org/10.1104/pp.110.163261>
- Yin, Y., Li, S., Liao, W., Lu, Q., Wen, X., & Lu, C. (2010). Photosystem II photochemistry, photoinhibition, and the xanthophyll cycle in heat-stressed rice leaves. *Journal of Plant Physiology* . <https://doi.org/10.1016/j.jplph.2009.12.021>

Zhang, P., Wang, R., Ju, Q., Li, W., Tran, L. S. P., & Xu, J. (2019). The R2R3-MYB transcription factor MYB49 regulates cadmium accumulation. *Plant Physiology* . <https://doi.org/10.1104/pp.18.01380>

Zhou, Z. S., Yang, S. N., Li, H., Zhu, C. C., Liu, Z. P., & Yang, Z. M. (2013). Molecular dissection of mercury-responsive transcriptome and sense/antisense genes in *Medicago truncatula* . *Journal of Hazardous Materials* . <https://doi.org/10.1016/j.jhazmat.2013.02.011>

Table 1. Concentration of ascorbic acid (ASA), reduced (GSH) and oxidized (GSSG) glutathione (in nmol g⁻¹ FW) measu

SHOOTS

ROOTS

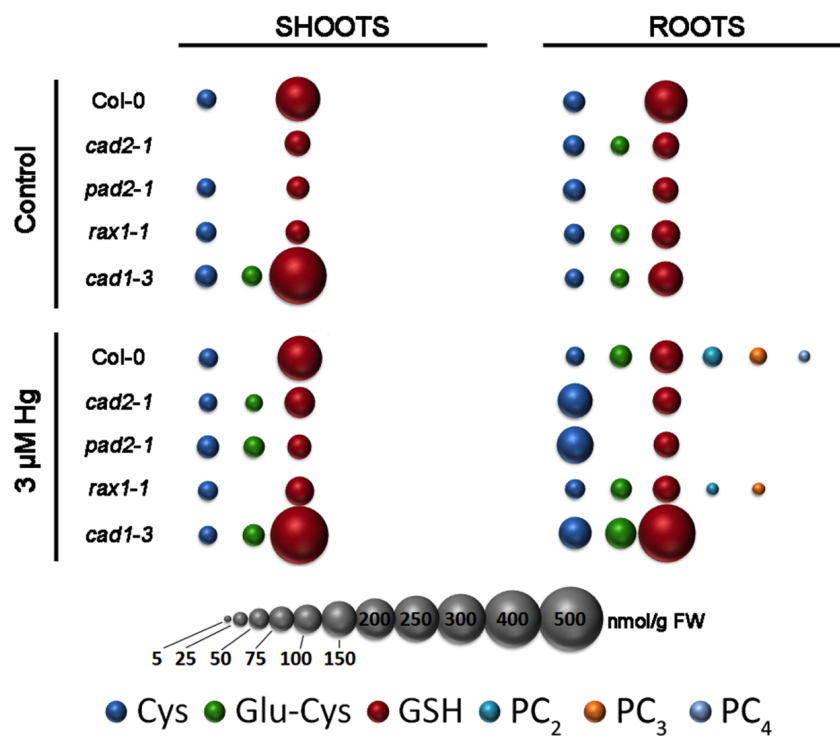


Fig.1 Summary of HPLC analysis of biothiol concentrations in shoots and roots (in $\text{nmol}\cdot\text{g}^{-1}$ FW) in wild type (Col-0), *cad2-1*, *pad2-1*, *rax1-1* and *cad1-3* *Arabidopsis thaliana* treated with 0 and 3 μM Hg for 72 h. Different biothiols are represented by spheres with different colours, with sphere diameters proportional to concentrations found. The concentration-to-volume scale is represented by the grey spheres at the bottom. For statistics and complete description of concentration values, please see Supplementary Table 1.

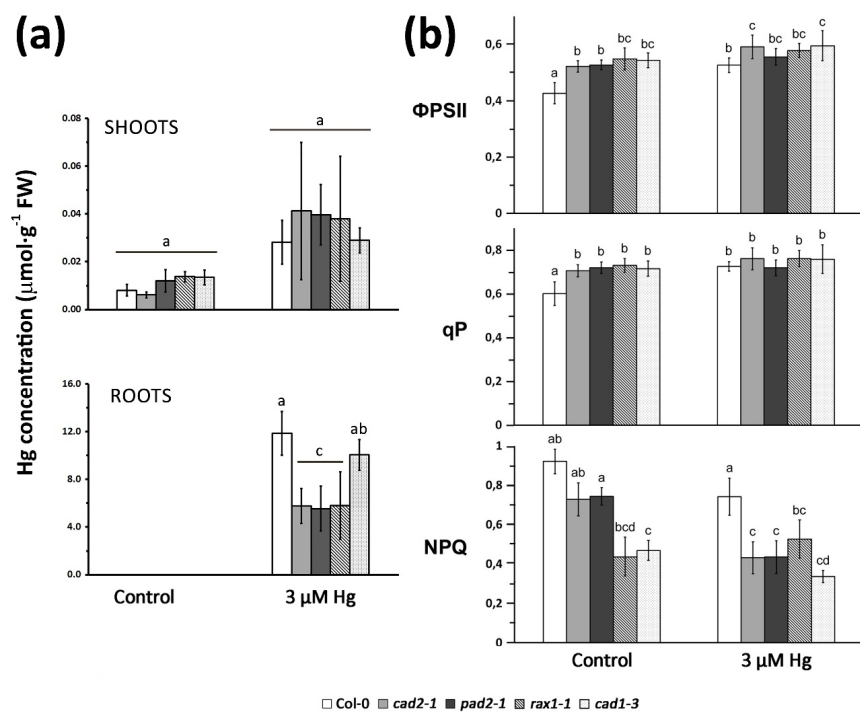


Fig. 2 (a) Mercury concentrations (in $\mu\text{mol}\cdot\text{g}^{-1}$ FW) in roots and shoots, and (n = 4) **(b)** chlorophyll fluorescence parameters in wild type (Col-0), *cad2-1*, *pad2-1*, *rax1-1* and *cad1-3* *Arabidopsis thaliana* treated with 0 and 3 μM Hg for 72 h: PSII efficiency (Φ_{PSII}), photochemical quenching (q_P) and non-photochemical quenching (NPQ) (n = 8). Different letters denote significant differences at $p < 0.05$

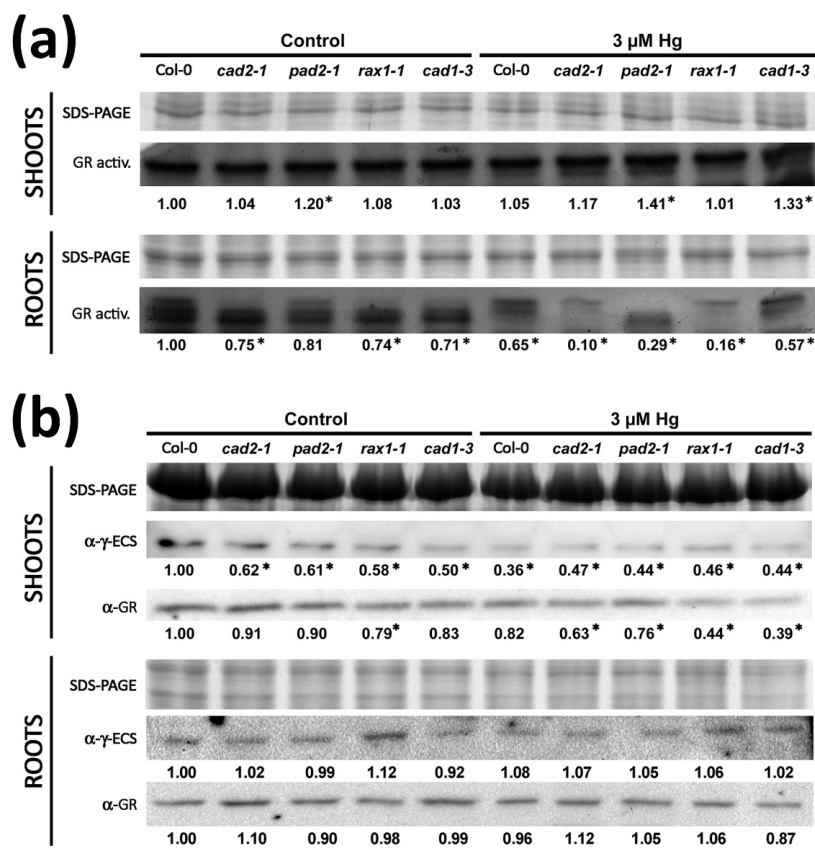


Fig. 3 (a) Glutathione reductase (GR) *in gel* activity, and **(b)** γ -glutamylcysteine synthetase (γ ECS) and glutathione reductase (GR) immunodetection in wild type (Col-0), *cad2-1*, *pad2-1*, *rax1-1* and *cad1-3* *Arabidopsis thaliana* treated with 0 and 3 μ M Hg for 72 h. Coomassie-blue staining was used to assure an equivalent protein loading of samples. Numbers represent the fold-change relative to the control Col-0, with asterisks marking decreases and decreases \geq 20%.

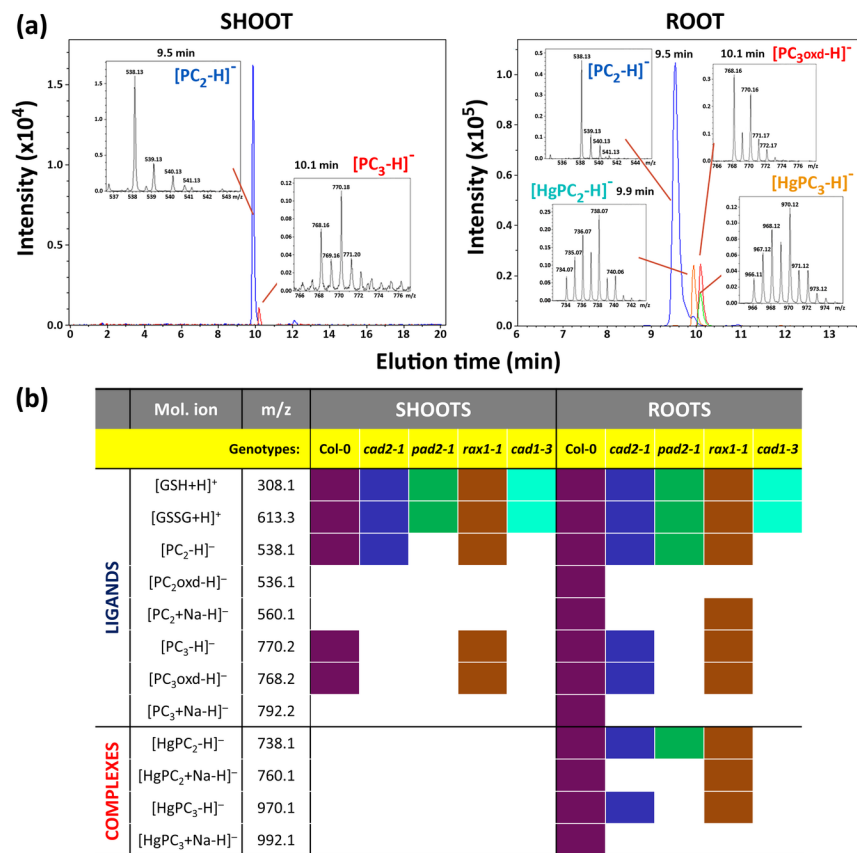


Fig. 4. PCs and Hg-PC complexes detected by HPLC-ESI-MS(TOF). **(a)** Examples of free PCs and Hg-PCs found in shoots and roots of Col-0 plants exposed to 3 μ M Hg for 72 h. Chromatographs and characteristic MS spectra of several molecular ions are shown (in negative mode). **(b)** Summary table describing the different molecular ions of biothiol ligands and Hg-PC complexes detected in shoots and roots of all *Arabidopsis* genotypes treated with 3 μ M Hg for 72 h. HPLC-ESI-MS(TOF) was carried out in negative and positive modes, and major detected molecular ions (m/z) are shown.

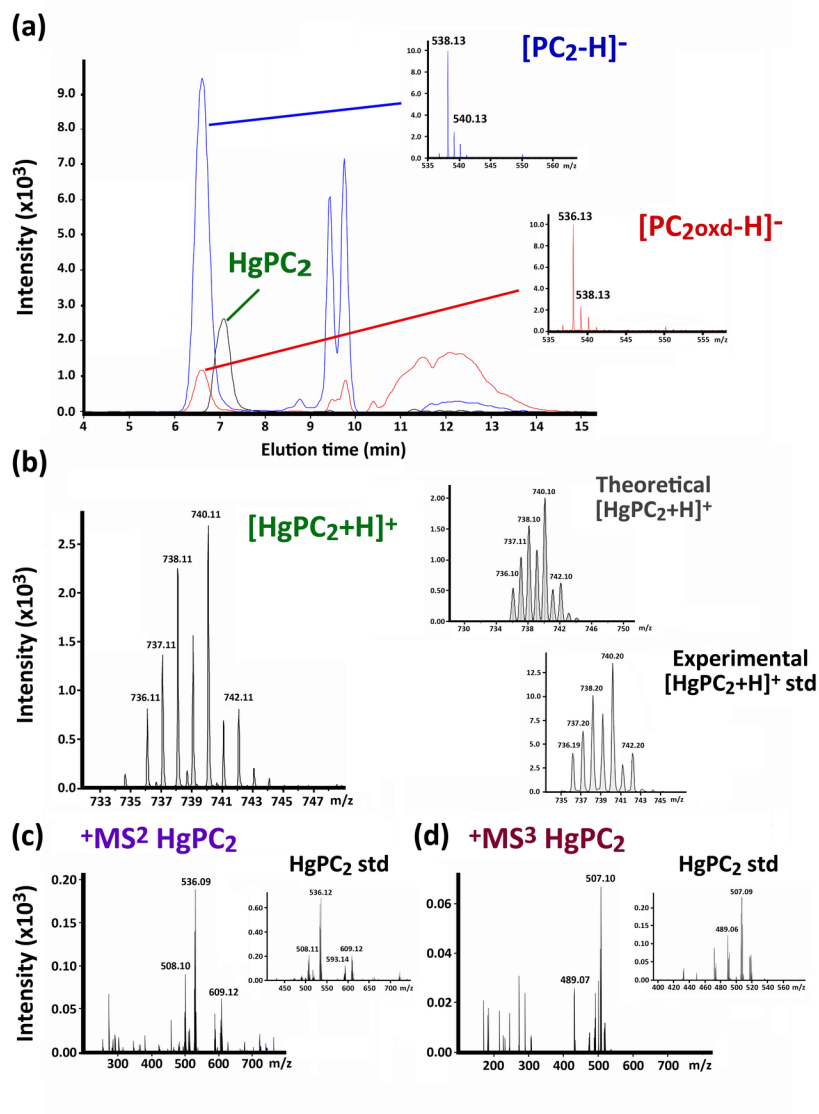


Fig. 5 HPLC-ESI-MS(TOF) analysis of PC and Hg-biothiol complexes in *Arabidopsis* Col-0 xylem sap. **(a)** Chromatographic profile of reduced PC₂, oxidized (PC₂oxd), and HgPC₂ detected in the xylem samples (in negative mode). **(b)** [HgPC₂+H]⁺ Molecular ion distribution (in m/z) compared with the theoretical one and a standard complex, prepared by mixing PC₂:HgCl₂ at 10:10 μM ratio (in positive mode). **(c)** and **(d)** MS² and MS³ fragmentation profiles of [HgPC₂+H]⁺, compared with those obtained using a standard PC₂:HgCl₂ mixture (insets), all in positive mode.

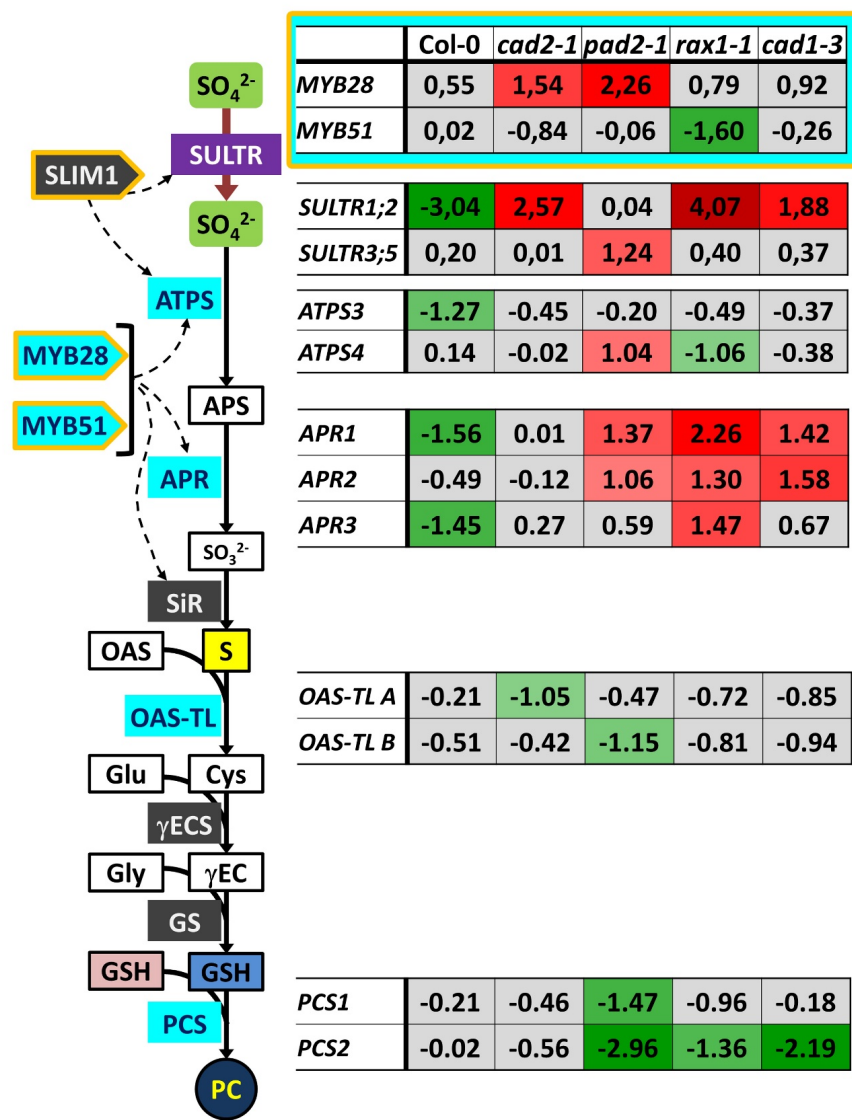


Fig. 6. Shoot transcriptional qRT-PCR profile of selected genes related to sulphur metabolism, using Col-0, *cad2-1*, *pad2-1*, *rax1-1* and *cad1-3* *Arabidopsis* treated with 0 or 3 μ M Hg for 72 h. Values are presented as log₂-fold change of Hg-treated plants relative to control plants of each genotype. Statistical differences with Col-0 (at $p < 0.05$) are represented as red and green boxes for over- and down-regulated genes, respectively. Grey boxes indicate no statistical differences. Data of genes encoding transcription factors () are shown in the inset box (). Light blue boxes also highlight genes differentially expressed. See quantitative values and statistics in Supplementary Table 3.

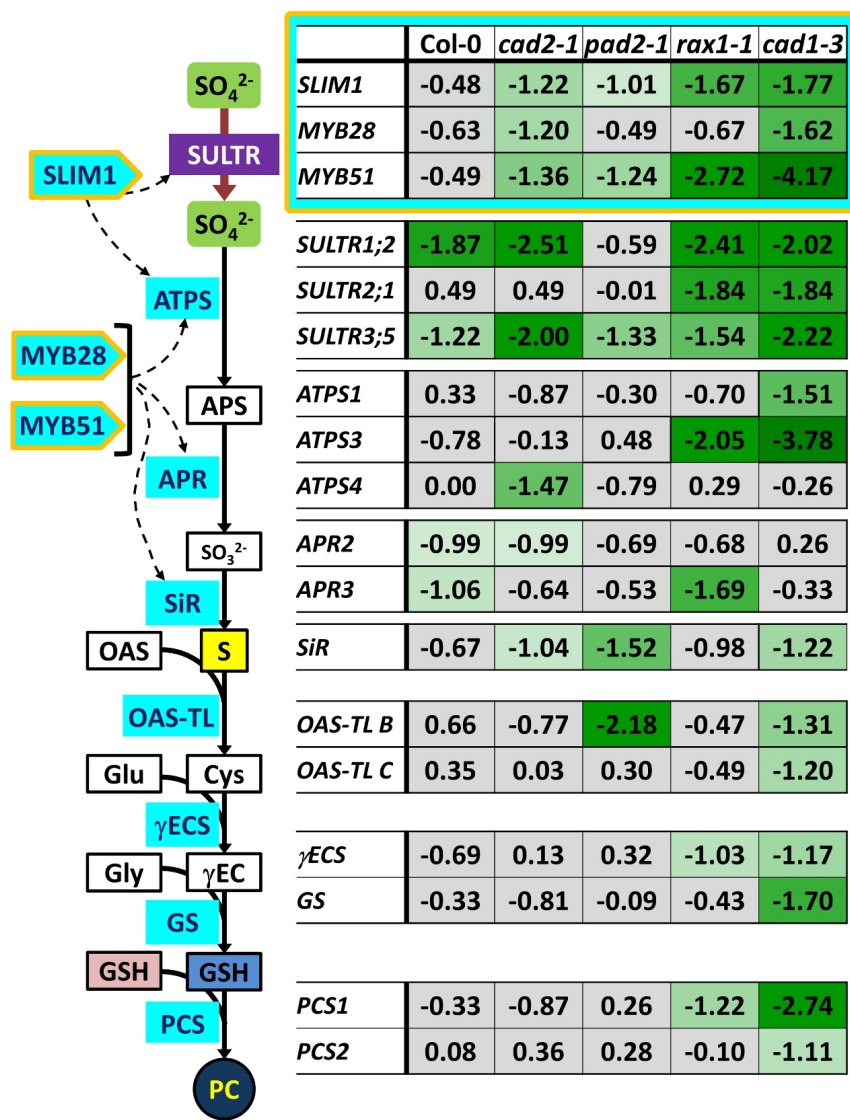


Fig. 7. Root transcriptional qRT-PCR profile of selected genes related to sulphur metabolism in Col-0, *cad2-1*, *pad2-1*, *rax1-1* and *cad1-3* *Arabidopsis* treated with 0 or 3 μ M Hg for 72 h. Values are presented as \log_2 -fold change of Hg-treated plants relative to control plants of each genotype. Statistically down-regulated genes when compared to Col-0 (at $p < 0.05$) are represented as green boxes, whereas grey boxes indicate no statistical difference. Data of genes encoding transcription factors () are shown in the inset box (). Light blue boxes highlight genes differentially expressed. See quantitative values and statistics in Supplementary Table 4.